AD

TECHNICAL REPORT ARCCB-TR-01004

MODELING PRESSURE VESSEL TOUGHNESS WITH VARIOUS SMALL SPECIMENS

EDWARD TROIANO
JOHN H. UNDERWOOD
CHARLES MOSSEY

FEBRUARY 2001

US ARMY ARMAMENT RESEARCH,
DEVELOPMENT AND ENGINEERING CENTER
CLOSE COMBAT ARMAMENTS CENTER
BENÉT LABORATORIES
WATERVLIET, N.Y. 12189-4050

DISCLAIMER

The findings in this report are not to be construed as an official Department of the Army position unless so designated by other authorized documents.

The use of trade name(s) and/or manufacturer(s) does not constitute an official endorsement or approval.

DESTRUCTION NOTICE

For classified documents, follow the procedures in DoD 5200.22-M, Industrial Security Manual, Section II-19, or DoD 5200.1-R, Information Security Program Regulation, Chapter IX.

For unclassified, limited documents, destroy by any method that will prevent disclosure of contents or reconstruction of the document.

For unclassified, unlimited documents, destroy when the report is no longer needed. Do not return it to the originator.

REPORT DOCUMENTATION PAGE

Form Approved
OMB No. 0704-0188

1. AGENCY USE ONLY *(Leave blank)*	2. REPORT DATE	3. REPORT TYPE AND DATES COVERED
	February 2001	Final

4. TITLE AND SUBTITLE

MODELING PRESSURE VESSEL TOUGHNESS
WITH VARIOUS SMALL SPECIMENS

5. FUNDING NUMBERS

AMCMS No. 6226.24.H180.0
PRON No. APPLIEDORDNA

6. AUTHOR(S)

Edward Troiano, John H. Underwood, and Charles Mossey

7. PERFORMING ORGANIZATION NAME(S) AND ADDRESS(ES)

U.S. Army ARDEC
Benet Laboratories, AMSTA-AR-CCB-O
Watervliet, NY 12189-4050

8. PERFORMING ORGANIZATION REPORT NUMBER

ARCCB-TR-01004

9. SPONSORING / MONITORING AGENCY NAME(S) AND ADDRESS(ES)

U.S. Army ARDEC
Close Combat Armaments Center
Picatinny Arsenal, NJ 07806-5000

10. SPONSORING / MONITORING AGENCY REPORT NUMBER

11. SUPPLEMENTARY NOTES

Presented at the 4th ASTM Symposium on Small Specimen Test Techniques, Reno, NV, 23-25 January 2001.
Published in ASTM STP.

12a. DISTRIBUTION / AVAILABILITY STATEMENT

Approved for public release; distribution unlimited.

12b. DISTRIBUTION CODE

13. ABSTRACT *(Maximum 200 words)*

Specimen configuration and size are often secondary considerations when performing fracture toughness tests. Typically the user will select a specimen geometry and size that are compatible with the material configuration, the type and size of the loading machine, and the clevises that are available. In the work here, special consideration is given to identifying the best configuration for measuring the fracture toughness of an internally-loaded pressure vessel. The work utilizes the Bowie and Freese stress intensity factor, K, for a pressurized cylinder over a wide range of crack lengths and cylinder wall ratios, with K normalized by von Mises combined stresses and remaining ligament ($K/\sigma_{VM}(w\text{-}a)^{1/2}$). This normalized K, when compared to the normalized K for the single-edge notched bend, SEN(B), the compact tension, C(T), and the middle tension, M(T), clearly indicates that depending on the a/w ratio, each of the specimens provides an optimum location where it can be used to model the pressure vessel. For intermediate a/w, as recommended by ASTM Test Method for Plane-Strain Fracture Toughness of Metallic Materials (E399), all of the specimens investigated distinctly under-predict the actual toughness of the pressure vessel. For the case of the pressure vessel with a wall ratio (w) of two, an under-prediction in toughness of 35% is predicted for the SEN(B) and M(T) specimens, and a 47% under-prediction is predicted for the C(T) specimen (at a/w = 0.5). Experiments were conducted on ASTM A723 steel (yield strength = 1125 MPa) at a/w ratios of 0.2, 0.467, 0.6, and 0.8 for the SEN(B), C(T), and M(T) specimens. The remaining ligament ($w\text{-}a$) was held constant at 8-mm (in order to match observations of previous pressure vessel failures). Specimen sizes were w = 10-mm, 15-mm, 20-mm, and 40-mm. Experimental results clearly show the trend predicted.

14. SUBJECT TERMS
Fracture Toughness, von Mises Stresses,
Pressure Vessels, Geometry Effects

15. NUMBER OF PAGES
13

16. PRICE CODE

17. SECURITY CLASSIFICATION OF REPORT	18. SECURITY CLASSIFICATION OF THIS PAGE	19. SECURITY CLASSIFICATION OF ABSTRACT	20. LIMITATION OF ABSTRACT
UNCLASSIFIED	UNCLASSIFIED	UNCLASSIFIED	UL

TABLE OF CONTENTS

TABLES

LIST OF ILLUSTRATIONS

INTRODUCTION

Fracture mechanics suggests that two cracks of similar size, in the same material, should respond in a similar fashion if they are subject to the same stress intensity, *K*. If one crack grows as a result of a given applied stress the other crack should also, irrespective of the size or shape of the body surrounding the crack. The work presented in this report combines the key parameters of stress intensity, von Mises combined stress, and remaining ligament into a "normalized" toughness. Then this toughness is compared as a function of normalized crack length, *a/w*, for pressure vessels with wall ratios of 1.75, 2.00, and 2.25, and for the compact tension, C(T), single-edge notched bend, SEN(B), and middle tension, M(T), specimens. The various geometries and loading utilized can be observed in Figure 1. Due to size limitations, the specimens for the study were taken in the LR orientation. Prior experience with this material, heat treatment, and processing has shown little directionality effect. Although this is not typically the crack plane of primary interest in pressurized vessels, it does provide enough information for proving the theory presented. Note in Figure 1 the significantly different stress states that are induced as a result of the applied loading. In this figure the stresses that result in self-similar cracking, σ_y, and off-axis cracking, σ_x, are defined for each of the geometries being studied. No bending is present in either the pressure vessel or the M(T) specimen, and the stress induced is a result of only normal loading. However, for the SEN(B) specimen, the stresses are the result of only bending loads; and for the C(T) specimen, the stresses are the result of a combination of bending and normal loading. In all cases, the through-thickness stress, σ_z, was assumed to be negligible and was omitted. The main focus of this study is to model actual final failure conditions of pressure vessels. Underwood et al. (ref 1) have provided a summary of prior final failure events for several pressure vessels with different wall ratios. These results can be seen in Table 1. The results are the averages for deep surface cracks emanating from the bore of the pressure vessel.

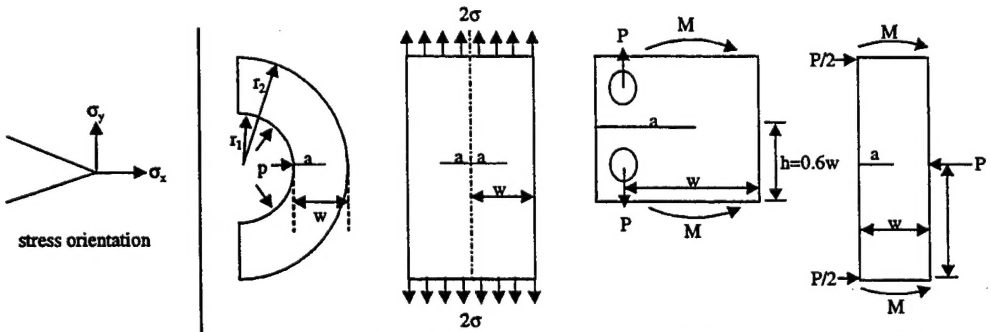

ligament stress	pressure vessel	M(T)	C(T)	SEN(B)
σ_x	-p	σ	$6M/Bh^2$	$6M/Bh^2$
σ_y	$pr_2/(w-a)$	$\sigma w/(w-a)$	$P/B(w-a)+6M/B(w-a)^2$	$6M/B(w-a)^2$
σ_z	0	0	0	0
M	---	---	P[a+(w-a)/2]	Pw

Figure 1. Ligament stresses for specimens investigated.

Table 1. Average Yield-Before-Break Failure Conditions of Pressure Vessels with a Surface Crack at the Inner Radius

Wall Ratio	Yield Strength (MPa)	Fracture Toughness (MPa $m^{1/2}$)	$(w-a)_c$ (mm)	a/w
1.90	1000	164	7	0.83
2.25	1090	187	8	0.89
1.79	1220	170	9	0.85
		Average	8	0.86

The average remaining ligament for the deep-cracked pressure vessels was 8-mm (at failure), with considerable plastic yielding accompanying the failure. The plan of this investigation was to use this 8-mm remaining ligament in various fracture specimen configurations with a range of crack depths in order to model the final failure behavior of thick-walled pressure vessels. The various specimen geometries, sizes, and related crack lengths were then set according to Table 2.

Table 2. Specimen Size and Configuration

Geometry	W (mm)	$(w\text{-}a)_{nominal}$ (mm)	a/w
C(T), SEN(B), M(T)	10	8	0.200
	15	8	0.467
	20	8	0.600
	40	8	0.800

Note that since the remaining ligament was previously set at a nominal 8-mm, the tests involved short crack lengths in the small specimens, moderate crack lengths in the mid-sized specimens, and large crack lengths in the larger specimens.

ANALYSIS

The following section describes the analysis for predicting the "normalized" toughness of each of the geometries investigated.

Pressure Vessel

Boundary collocation K results developed by Bowie and Freese (ref 2) and further improved by Andrasic and Parker (ref 3) provide a wide array of stress intensity solutions as a function of wall ratio for an internally pressurized cylinder with a crack emanating from the bore of the pressure vessel. These results fall short, however, because neither fits the solutions to the deep-crack limit, which is of great interest for predicting final failure of thick-walled pressure vessels, especially in this case where the average a/w is 0.86 at failure. Underwood and Witherell (ref 4) have added to the original work by Bowie and Freese to include the deep-crack limit solution, as provided in Reference 5. The K solution for a pressurized vessel (ref 4) is

$$\frac{K}{3.97p}\frac{\left(\left(1-a/w\right)^{1/2}\left(\frac{W^2-1}{W^2}\right)\right)}{\sqrt{a}}=C_{PV}=C_1\frac{a}{w}+C_2\left(\frac{a}{w}\right)^2+C_3\left(\frac{a}{w}\right)^3+C_4\left(\frac{a}{w}\right)^4 \quad (1)$$

where a is the crack length, w is the wall thickness (r_2-r_1), p is the internal pressure, W is the wall ratio (r_2/r_1), and $C_1 \ldots C_n$ are the unique coefficients for each wall ratio investigated. Through some simple algebraic manipulations, one can rewrite the expression as

$$K = pf_{PV}\sqrt{w-a} \quad (2)$$

where

$$f_{PV}=3.97C_{PV}\frac{\sqrt{a/w}}{\left(1-a/w\right)\left(\frac{W^2-1}{W^2}\right)} \quad (3)$$

Using equation (2), along with expressions for σ_x, the stress component that induces off-axis cracking, and σ_y, the stress component that induces self-similar cracking, in Figure 1, we can write the normalized K expressions in terms of σ_x and σ_y as follows:

$$\frac{K}{\sigma_x\sqrt{w-a}}=-f_{PV} \quad (4)$$

and

$$\frac{K}{\sigma_y\sqrt{w-a}}=f_{PV}\frac{1-a/w}{\left(\frac{1}{1-a/w}\right)} \quad (5)$$

Compact Tension Specimen

The compact tension specimen is analyzed in a fashion similar to that presented above. In this case, the K expression as defined in E399 is

$$K=\frac{p}{B\sqrt{w}}f_c \quad (6)$$

where p is the pin load, B is the specimen thickness, w is the width of the specimen, and f_c is defined as

$$f_c = \frac{\left(2+a/w\right)\left(0.886+4.64\,a/w-13.32\,a^2/w^2+14.72\,a^3/w^3-5.6\,a^4/w^4\right)}{\left(1-a/w\right)^{3/2}} \tag{7}$$

which is valid on the region $0.2 < a/w < 1$. Now, using equation (6), along with the expression for σ_x and σ_y for the compact tension specimen as defined in Figure 1, we can write the normalized K expressions as

$$\frac{K}{\sigma_x\sqrt{w-a}} = \frac{f_c}{16.67\,a/w\sqrt{1-a/w}} \tag{8}$$

and

$$\frac{K}{\sigma_y\sqrt{w-a}} = fc\sqrt{1-a/w}\left(\frac{1-a/w}{3\left(1+a/w\right)}+1\right) \tag{9}$$

Single-Edge Notch Bend Specimen

The K expression, as defined in E399, for the single-edge notched beam is

$$K = \frac{pS}{Bw^{3/2}} f_B \tag{10}$$

where p, B, and w are previously defined, S is the span of the pin supports, usually $4w$, and f_B is defined as

$$f_B = \frac{\left(3\sqrt{a/w}\right)\left(1.99-\left(a/w\right)\left(1-a/w\right)\left(2.15-3.93\,a/w+2.7\,a^2/w^2\right)\right)}{2\left(1+2\,a/w\right)\left(1-a/w\right)^{3/2}} \tag{11}$$

which is valid on the region $0 < a/w < 1$. Using equation (10), along with the expression for σ_x and σ_y for the single-edge notched beam specimen as defined in Figure 1, we can write the normalized K expressions as

$$\frac{K}{\sigma_x\sqrt{w-a}} = \frac{f_B}{0.375\sqrt{1-a/w}} \tag{12}$$

and

$$\frac{K}{\sigma_y\sqrt{w-a}} = 0.667 f_B \left(1-a/w\right)^{3/2} \tag{13}$$

Middle Tension Specimen

The K expression, as defined in Reference 4, for the middle tension specimen is

$$K = \frac{p}{2Bw}\sqrt{\pi a}\, f_M \tag{14}$$

where p, B, and w and a are previously defined, and f_M is defined as

$$f_M = \frac{1-0.5\,a/w+0.326\left(a/w\right)^2}{\sqrt{1-a/w}} \tag{15}$$

which is valid from $0 < a/w < 1$. Using equation (14) along with the expression for σ_x and σ_y for the middle tension specimen as defined in Figure 1, we can write the normalized K expressions as

$$\frac{K}{\sigma_x\sqrt{w-a}} = \frac{-f_M\sqrt{\pi}\sqrt{a/w}}{\sqrt{1-a/w}} \tag{16}$$

and

$$\frac{K}{\sigma_y\sqrt{w-a}} = f_M\sqrt{\pi}\sqrt{a/w}\sqrt{1-a/w} \tag{17}$$

Summary of Analysis

The normalized K expressions for the geometries presented are plotted in Figure 2 for the off-axis stresses, (we will hereafter set $K_{\sigma x} = K/\sigma_x(w\text{-}a)^{1/2}$) and in Figure 3 for the self-similar stresses we will hereafter set $K_{\sigma y} = K/\sigma_y(w\text{-}a)^{1/2}$). In both figures, three wall ratios were analyzed, $W = 1.75$, 2.00, and 2.25. The next step is to combine the normalized K with the von Mises equivalent stress for yielding

$$\frac{K}{\sigma_{VM}\sqrt{w-a}} = \sqrt{K_{\sigma x}^2 + K_{\sigma y}^2 - K_{\sigma x}K_{\sigma y}} \tag{18}$$

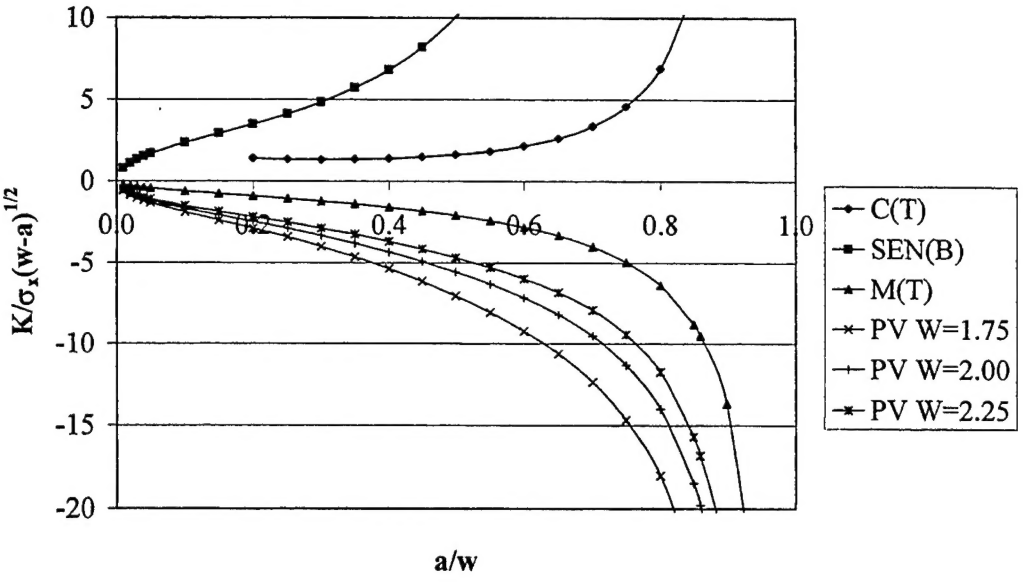

Figure 2. Normalized off-axis stress intensity for various configurations.

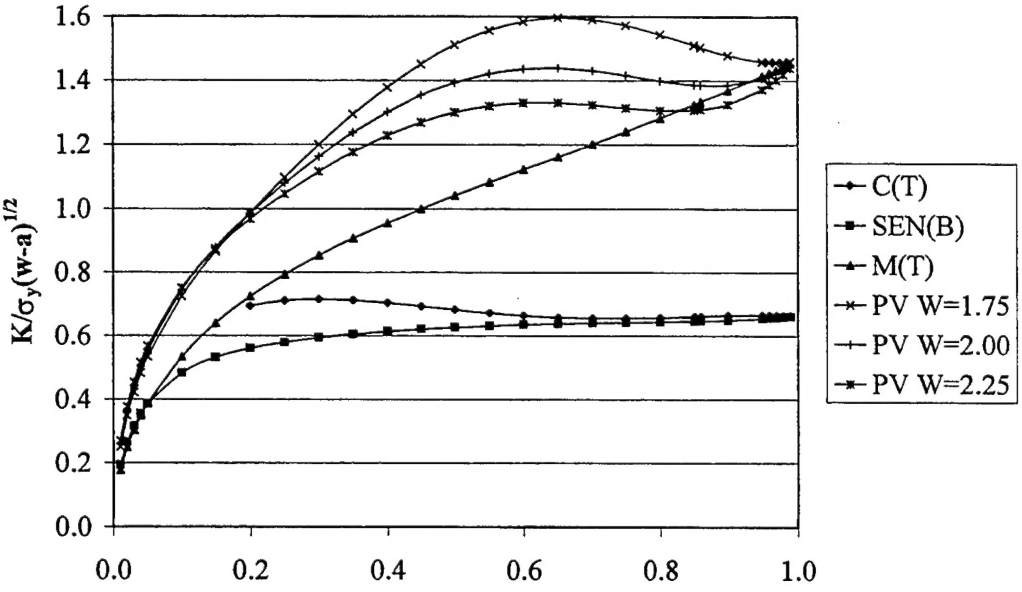

Figure 3. Normalized self-similar stress intensity for various configurations.

These results, for the SEN(B), C(T), M(T), and three different wall ratio pressure vessels are graphically presented in Figure 4. The results suggest that for *a/w* of 0.2, the C(T) geometry closely approximates the normalized toughness of all three wall ratio pressure vessels, whereas the SEN(B) and M(T) specimens under-predict the toughness. At a moderate length *a/w* of 0.5, all of the specimens significantly under-predict the toughness of the pressure vessels. Also, at a large *a/w* of 0.85 (approximately the same as the *a/w* measured in Reference 1), the M(T) specimen toughness is approaching that of the pressure vessels, and the SEN(B) and C(T) specimens are less than 50% of that predicted for the M(T) and the pressure vessels.

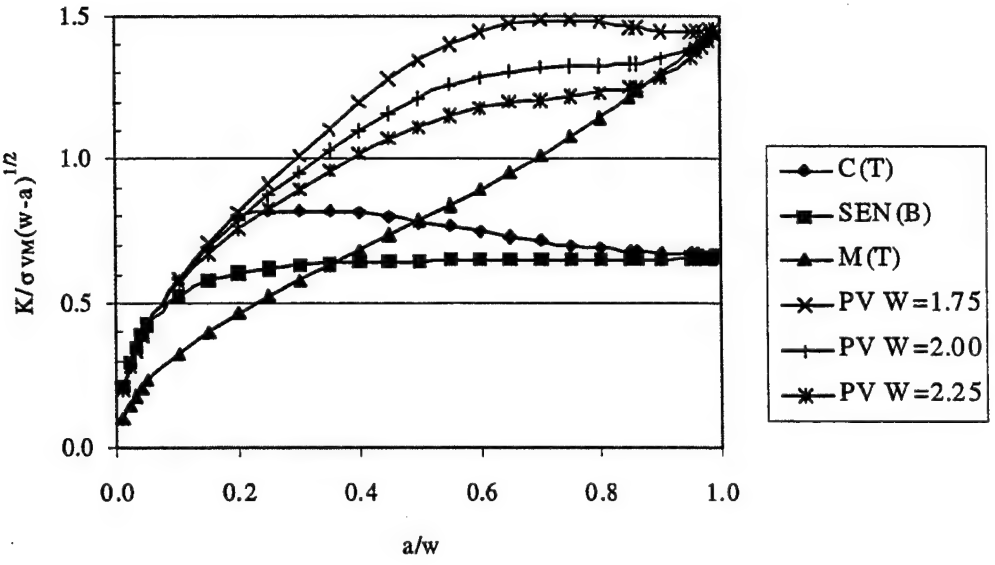

Figure 4. Normalized von Mises stress intensity for various configurations.

Note that in the limit as *a/w* tends toward zero, the M(T) and SEN(B) tend toward the same limit as the pressure vessels. This condition is interesting, but not of much interest here. For the deep-crack limit, which is of primary interest, the M(T) specimen tends toward the same limits as the pressure vessels, whereas the C(T) and SEN(B) do not. This similarity between the pressure vessel and M(T) specimen may be related to how a pressure vessel and the M(T) specimen respond to applied pressure loading (see Figure 5). The case of a pressure vessel with cracks emanating from the bore surface, with pressure both in the bore and in the cracks, is analogous to the same pressure vessel with an external applied pressure. This condition is analogous to the M(T) specimen with an external applied pressure. In the deep-crack limit, all three scenarios sketched in Figure 5 are identical.

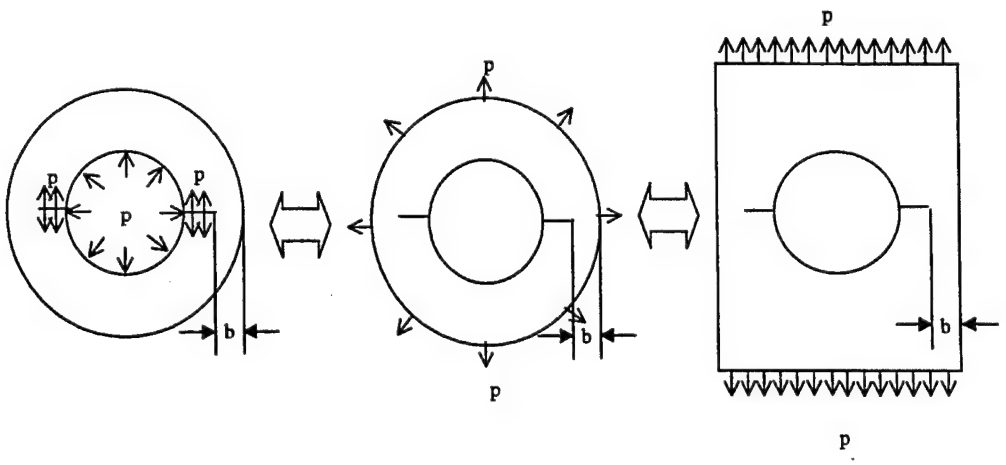

Figure 5. Analogy between internally pressurized cylinder and remotely loaded hole in plate.

EXPERIMENTAL RESULTS

Experiments were conducted on A723 Grade 2 pressure vessel quality steel, to validate the analysis discussed here. Properties of the steel appear in Table 3.

Table 3. Mechanical Properties of A723 Grade 2 Pressure Vessel Quality Steel

Yield Strength (MPa)	Ultimate Tensile Strength (MPa)	Reduction-in-Area (%)	Elongation (%)	Charpy Impact Energy (J, -40°C)	Young's Modulus (GPa)
1125	1235	54	15	57	205

All of the specimens were machined from the same pressure vessel so as to eliminate any slight anomalies that might exist.

Compact Tension Specimen and Single-Edge Notch Beam Specimen

Testing was conducted on these specimens (C(T) and SEN(B)) according to ASTM Test Method for J-Integral Characterization of Fracture Toughness (E1737). This test method was chosen because it allows for an accurate measure of elastic-plastic toughness at any point, for a continuous measure of load and crack extension, and for results that can easily be converted at any point by the well-known equation

$$K = \sqrt{\frac{J_i E}{(1-\upsilon^2)}} \tag{19}$$

where E is the elastic modulus, υ is Poisson's Ratio ($\upsilon = 0.3$), and J_i is the elastic-plastic toughness at the point of interest.

The compliance unloading method for determining crack extension was utilized, and an accurate real time measure of J, load and crack extension was obtained. This information will be useful for comparing these results to the M(T) specimen.

Middle Tension Specimen

Since there is no method available for directly measuring the J-integral for the M(T) specimen, an alternate method for measuring the toughness of this geometry was sought. Original work by Rice et al. (ref 6), which was later modified and refined by Ernst et al. (ref 7) to accommodate the elastic and plastic η factor, defines the J-integral for an internally notched plate in tension as

$$J_i = G + \frac{1}{b}[\eta \int_0^{\delta_{plastic}} P d\delta_{plastic} - P\delta_{plastic}] \tag{20}$$

where G is the elastic or Griffith energy, which is defined as

$$G = \frac{K^2(1-\upsilon^2)}{E} \tag{21}$$

and the second term is the nonlinear portion, or plastic energy. This equation allows for an accurate representation of the elastic-plastic toughness to be measured from a single load-displacement curve at any point of interest along the curve. Equation (19) is then utilized to convert to K.

Summary of Experimental Results

Results from the tests are clearly displayed in Figure 6. The K results in the figure were taken after 0.075-mm of crack extension. For the SEN(B) and C(T) specimens, this point was easily established because the compliance unloading procedure gave an accurate representation of Δa. Since no such record was available for the M(T) specimen, a simple offset rule was employed. It was assumed that since the material used was identical, then the shape of the load-displacement trace would be similar for each of the geometries. Also, since we knew the offset that was necessary for 0.075-mm of crack extension in the SEN(B) and C(T) specimens, we could utilize the same offset to approximate 0.075-mm of crack extension for the M(T) specimens. There are other more accurate methods for establishing this point, however it was not necessary in this case. Once the point was established, each of the traces was used to measure J and convert to K at Δa = 0.075-mm. The 0.075-mm of crack extension was chosen because it was felt that this amount of Δa could easily be monitored with the compliance unloading technique. If the Δa were any smaller, the inaccuracies with the technique might allow for too much variation in the analysis. Another interesting point is that the analysis is irrespective of the absolute amount of crack growth, and the reader can easily choose a different Δa for comparison. Note in Figure 6 the large amount of scatter, not only with the geometry, but also with size of the specimens when plotted in terms of K.

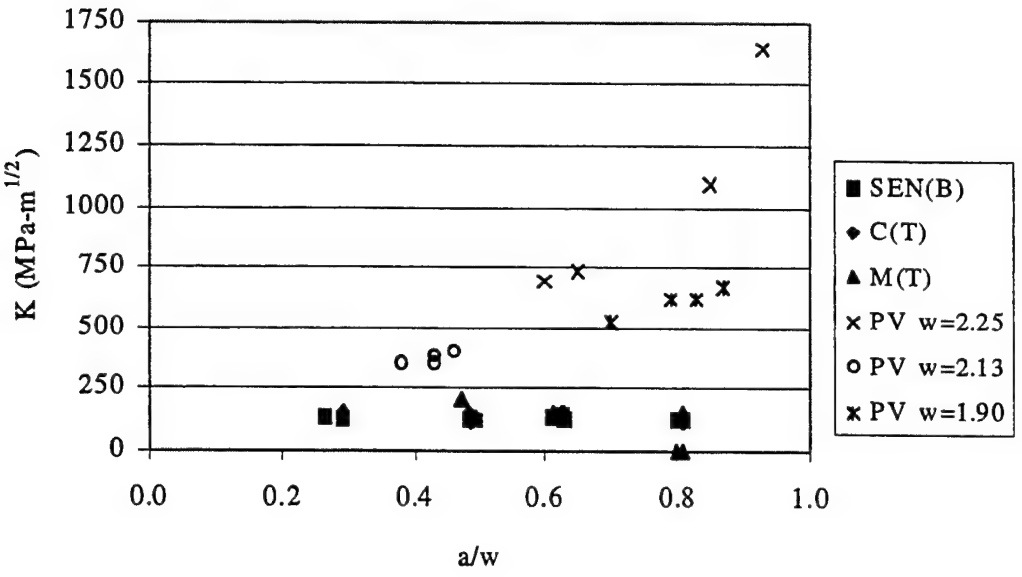

Figure 6. Calculated stress intensity for various configurations.

Knowing all the necessary data in equations (1), (6), (10), and (14), for the pressure vessel, C(T), SEN(B), and M(T) specimens, respectively, and also having all the necessary information for calculating the self-similar and off-axis stresses in Figure 1, we can easily evaluate the normalized toughness, $K/\sigma_{VM}(w\text{-}a)^{1/2}$, for each of the geometries. These results are displayed in Figure 7. Note the good agreement we obtain between the experimental (exp) and theoretical predictions.

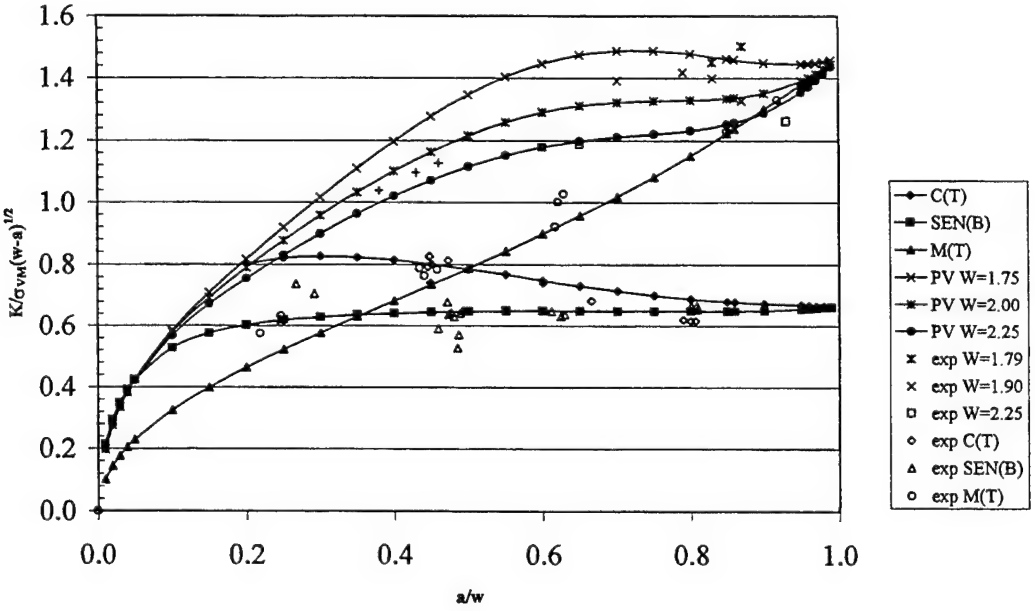

Figure 7. Theoretical and experimental stress intensities for various configurations.

CONCLUSIONS

- This technique can be utilized to select the best specimen configuration and crack length for predicting the toughness of a given material and structural configuration. If the user knows a few critical features such as the overall geometry, *a/w*, and the loading, an accurate prediction of the toughness can be made for that specific application.

- The technique is not dependent on material properties such as yield strength, and only considers the ratio of K to crack tip von Mises stresses and the remaining ligament. It is cautioned that this technique has been proven to be useful for relatively high-strength pressure vessel steel at a crack extension of 0.075-mm. Should the reader be interested in using this technique for other materials and structural configurations, they are cautioned to investigate which crack extension would be appropriate for their application.

- This method is general and simple, so it should be relatively easy to perform this type of analysis on a wide variety of structural configurations and geometries, other than those investigated here.

REFERENCES

1. Underwood, J.H., Farrara, R.A., and Audino, M.J., "Yield-Before-Break Fracture Mechanics Analysis of High-Strength Steel Pressure Vessels," *ASME Journal of Pressure Vessel Technology*, (R. Swinderman, Ed.), Vol. 117, 1995, pp. 79-84.

2. Bowie, O.L., and Freese, C.E., "Elastic Analysis for a Radial Crack in a Circular Ring," *Engineering Fracture Mechanics*, Vol. 4, 1972, pp. 315-321.

3. Andrasic, C.P., and Parker, A.P., "Dimensionless Stress Intensity Factors for Cracked Thick Cylinders under Polynomial Crack Face Loading," *Engineering Fracture Mechanics*, Vol. 19, 1984, pp. 187-193.

4. Underwood, J.H., and Witherell, M.D., "Stress Intensity Factor Solutions for Armament; Pressure Vessel and Composite Laminate Applications," *Proceedings of the 15th U.S. Army Symposium on Solid Mechanics*, 1999.

5. Tada, H., Paris, P.C., and Irwin, G.R., *The Stress Analysis of Cracks Handbook*, Paris Productions, St. Louis, 1985, p. 9.2.

6. Rice, J.R., Paris, P.C., and Merkle, J.G., "Some Further Results of *J*-Integral Analysis and Estimates," *Progress in Flaw Growth and Fracture Toughness Testing, ASTM STP 536*, American Society for Testing and Materials, 1973, pp.231-245.

7. Ernst, H.A., Paris, P.C., and Landes, J.D., "Estimations on *J*-Integral and Tearing Modulus from a Single Specimen Test Record," *Fracture Mechanics Thirteenth Conference, ASTM STP 743*, (Richard Roberts, Ed.), American Society for Testing and Materials, 1981, pp. 476-502.

TECHNICAL REPORT INTERNAL DISTRIBUTION LIST

	NO. OF COPIES
TECHNICAL LIBRARY ATTN: AMSTA-AR-CCB-O	5
TECHNICAL PUBLICATIONS & EDITING SECTION ATTN: AMSTA-AR-CCB-O	3
OPERATIONS DIRECTORATE ATTN: SIOWV-ODP-P	1
DIRECTOR, PROCUREMENT & CONTRACTING DIRECTORATE ATTN: SIOWV-PP	1
DIRECTOR, PRODUCT ASSURANCE & TEST DIRECTORATE ATTN: SIOWV-QA	1

NOTE: PLEASE NOTIFY DIRECTOR, BENÉT LABORATORIES, ATTN: AMSTA-AR-CCB-O OF ADDRESS CHANGES.

TECHNICAL REPORT EXTERNAL DISTRIBUTION LIST

	NO. OF COPIES
DEFENSE TECHNICAL INFO CENTER ATTN: DTIC-OCA (ACQUISITIONS) 8725 JOHN J. KINGMAN ROAD STE 0944 FT. BELVOIR, VA 22060-6218	2
COMMANDER U.S. ARMY ARDEC ATTN: AMSTA-AR-WEE, BLDG. 3022	1
AMSTA-AR-AET-O, BLDG. 183	1
AMSTA-AR-FSA, BLDG. 61	1
AMSTA-AR-FSX	1
AMSTA-AR-FSA-M, BLDG. 61 SO	1
AMSTA-AR-WEL-TL, BLDG. 59 PICATINNY ARSENAL, NJ 07806-5000	2
DIRECTOR U.S. ARMY RESEARCH LABORATORY ATTN: AMSRL-DD-T, BLDG. 305 ABERDEEN PROVING GROUND, MD 21005-5066	1
DIRECTOR U.S. ARMY RESEARCH LABORATORY ATTN: AMSRL-WM-MB (DR. B. BURNS) ABERDEEN PROVING GROUND, MD 21005-5066	1
COMMANDER U.S. ARMY RESEARCH OFFICE ATTN: TECHNICAL LIBRARIAN P.O. BOX 12211 4300 S. MIAMI BOULEVARD RESEARCH TRIANGLE PARK, NC 27709-2211	1
COMMANDER ROCK ISLAND ARSENAL ATTN: SIORI-SEM-L ROCK ISLAND, IL 61299-5001	1
COMMANDER U.S. ARMY TANK-AUTMV R&D COMMAND ATTN: AMSTA-DDL (TECH LIBRARY) WARREN, MI 48397-5000	1
COMMANDER U.S. MILITARY ACADEMY ATTN: DEPT OF CIVIL & MECH ENGR WEST POINT, NY 10966-1792	1
U.S. ARMY AVIATION AND MISSILE COM REDSTONE SCIENTIFIC INFO CENTER ATTN: AMSAM-RD-OB-R (DOCUMENTS) REDSTONE ARSENAL, AL 35898-5000	2
COMMANDER U.S. ARMY FOREIGN SCI & TECH CENTER ATTN: DRXST-SD 220 7TH STREET, N.E. CHARLOTTESVILLE, VA 22901	1

NOTE: PLEASE NOTIFY COMMANDER, ARMAMENT RESEARCH, DEVELOPMENT, AND ENGINEERING CENTER, BENÉT LABORATORIES, CCAC, U.S. ARMY TANK-AUTOMOTIVE AND ARMAMENTS COMMAND, AMSTA-AR-CCB-O, WATERVLIET, NY 12189-4050 OF ADDRESS CHANGES.